

## **Singlet oxygen generation by the genetically-encoded tag**

### **miniSOG**

Rubén Ruiz-González,<sup>1</sup> Aitziber L. Cortajarena,<sup>2,3</sup> Sara H. Mejias,<sup>2,3</sup> Montserrat Agut,<sup>1</sup> Santi Nonell<sup>1\*</sup>  
and Cristina Flors<sup>2\*</sup>

<sup>1</sup>Institut Químic de Sarrià, Universitat Ramon Llull, Via Augusta 390, E-08019, Barcelona, Spain

<sup>2</sup>IMDEA Nanociencia, C/ Faraday 9, Ciudad Universitaria de Cantoblanco, 28049 Madrid, Spain

<sup>3</sup>CNB-CSIC-IMDEA Nanociencia Associated Unit "Unidad de Nanobiotecnología", Ciudad Universitaria de Cantoblanco,  
28049 Madrid, Spain

#### **This file contains:**

- **Materials and Methods**
- **Deuterium isotope effect on the photooxidation of ADPA**
- **ADPA photooxidation studies**
- **Figures S1- S9**
- **Supporting references**

## Supporting Information

### Materials and Methods

#### *Chemical Compounds*

Uric Acid and Guanidinium Hydrochloride (Sigma). Flavin Mononucleotide (Chemochroma) and Anthracene-9,10-dipropionic acid disodium salt (Chemodex) were used as received. PBS or dPBS solutions were prepared dissolving the required amount of a PBS tablet (Sigma) in 100 mL milliQ water or deuterium oxide (Fluka). Phenalenone-2-sulfonate was resynthesized according to the published method in reference.<sup>1</sup>

#### *MiniSOG expression and purification*

The pBAD-Myc-HisA plasmid encoding miniSOG (from Tsien Lab) was transformed into *Escherichia coli* DH5 $\alpha$  cells. The expression and purification was performed in the darkness following minor modifications of the protocol described elsewhere.<sup>2</sup> One litre cell culture was grown from a single colony in LB media with 0.1% arabinose as inducing agent at 37 °C overnight. The cells were harvested by centrifugation and the pellets resuspended with lysis buffer (300 mM NaCl, 50 mM phosphate pH 7.4) supplemented with a protease inhibitor cocktail (Roche, Basel, Switzerland). Cells were lysed by sonication and the lysate was cleared by centrifugation during 30 min. at 4 °C and 45000 x g. His-tagged miniSOG was purified from the supernatant using a Cobalt-agarose affinity column (Jena bioscience, Jena, Germany). The eluted fractions with protein were dialyzed into 150 mM NaCl, 50 mM phosphate pH 7.4 (PBS buffer). A second Cobalt affinity column was run to ensure protein purity, which was determined by SDS-PAGE gel and MALDI-TOF mass spectrometry. Protein concentration was determined by measuring the absorbance at 280 nm, using extinction coefficients calculated from amino acid composition and absorbance at 448 nm using an extinction coefficient of 16760 M<sup>-1</sup>·cm<sup>-1</sup>.<sup>3</sup> The Trp81Phe miniSOG protein mutant was generated using the quick-change technique. The mutation was confirmed by sequencing. miniSOG (W81F) was expressed and purified as described above for the WT protein. For expression of a tagless miniSOG variant the miniSOG gene was amplified by PCR and recloned into a pPRO-EX-HTa-modified expression vector (Invitrogen), using the restriction sites BamHI and HindIII to create genes with an N-terminal His6-tag followed by a TEV cleavage site. The plasmids were transformed into *E. coli* C41 cells. Cells were grown at 37°C to an OD600 of 0.6-0.8, then the expression was induced with 0.6 mM IPTG and grown 5 h at 30°C. The protein is purified using the same protocol described above. Finally, the His-tag was cleaved by overnight TEV protease digestion at 4°C and the His-tag and the tagged protease removed by a second Cobalt affinity column.

#### *Photodynamic inactivation protocol*

Photodynamic inactivation experiments of *E. coli* strains BL21 (DE3) expressing TagRFP or DH5 $\alpha$  expressing miniSOG were carried out. Cell cultures in exponential growing phase were induced either with 50  $\mu$ M isopropyl  $\beta$ -D-1-thiogalactopyranoside (IPTG) or 0.1% arabinose for 1 h, respectively. After replacing the growth medium with PBS the cells were transferred to an optical non-treated sterile glass chamber and irradiated through the top of the chamber by means of a LED light source (Sorisa Photocare) using a 35 mW·cm<sup>-2</sup> fluence rate

## Supporting Information

either in the green for TagRFP ( $535 \pm 15$  nm) or in the blue for miniSOG ( $475 \pm 15$  nm). For CFU determination, irradiated/control sample aliquots was serially diluted, streaked on nutrient agar, and incubated in the dark for 18 h at 37 °C.

### *Protein denaturation protocol*

MiniSOG was adjusted to a concentration of 2.5  $\mu$ M in a 6 M solution of Gdn HCl (PBS or dPBS) according to a well-established protocol.<sup>4</sup> The solution was stirred over time and, periodically, absorption and fluorescence spectra were acquired in order to assess the degree of denaturation.

### *Spectroscopic measurements*

Absorption spectra were recorded on a Cary 6000i spectrophotometer (Varian, Palo Alto, CA). Fluorescence emission spectra were recorded in a Spex Fluoromax-4 spectrofluorometer (Horiba Jobin-Yvon, Edison, NJ). Fluorescence decays were recorded with a time-correlated single photon counting system (Fluotime 200, PicoQuant GmbH, Berlin, Germany) equipped with a red sensitive photomultiplier. Excitation was achieved by means of a 375 nm picosecond diode laser working at 10 MHz repetition rate. The counting frequency was always below 1%. Fluorescence lifetimes were analyzed using PicoQuant FluoFit 4.0 data analysis software. Transient absorption spectra were monitored by nanosecond laser flash photolysis using a Q-switched Nd-YAG laser (Surelite I-10, Continuum) coupled to an OPO laser (SL OPO, Continuum; 5 ns pulse width, 1-10 mJ per pulse) with right-angle geometry and an analyzing beam produced by a Xe lamp (PTI, 75 W) in combination with a dual-grating monochromator (mod. 101, PTI) coupled to a photomultiplier (Hamamatsu R928). Kinetic analysis of the individual transients was performed with software developed in our laboratory. Excitation wavelengths were 355 or 475 nm depending on the experiment.

### *Singlet oxygen quantum yield measurements*

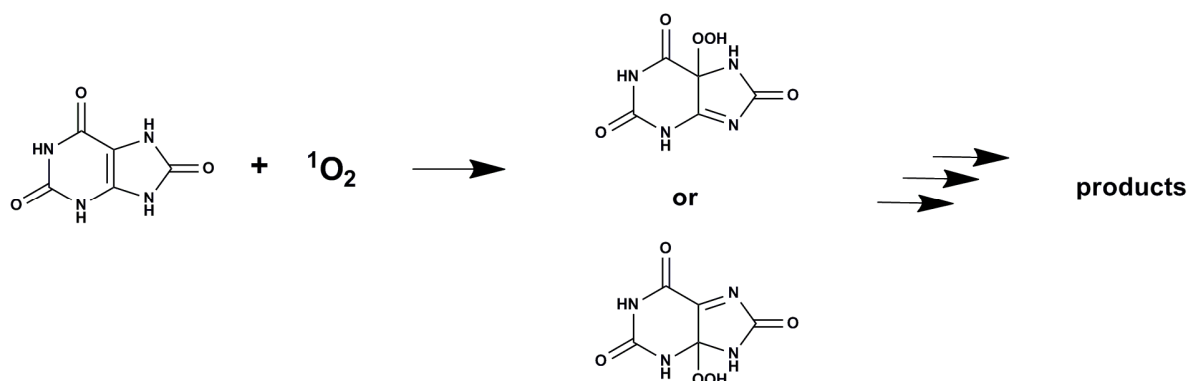
Direct  $^1\text{O}_2$  luminescence was detected by means of a customized PicoQuant Fluotime 200 system described in detail elsewhere.<sup>5</sup> Briefly, a diode-pumped pulsed Nd:YAG laser (FTSS355-Q, Crystal Laser, Berlin, Germany) working at 10 kHz repetition rate at 532 nm (12 mW, 1.2  $\mu$ J per pulse) was used for excitation. A 1064 nm rugate notch filter (Edmund Optics, U.K.) was placed at the exit port of the laser to remove any residual component of its fundamental emission in the near-IR region. The luminescence exiting from the side of the sample was filtered by two long-pass filters of 355 and 532 nm (Edmund Optics, York, U.K.) and two narrow bandpass filters at 1275 nm (NB-1270-010, Spectrogon, Sweden; bk-1270-70-B, bk Interferenzoptik, Germany) to remove any scattered laser radiation. A near-IR sensitive photomultiplier tube assembly (H9170-45, Hamamatsu Photonics Hamamatsu City, Japan) was used as the detector at the exit port of the monochromator. Photon counting was achieved with a multichannel scaler (PicoQuant's Nanoharp 250). The time-resolved emission signals were analyzed using the PicoQuant FluoFit 4.0 data analysis software to extract the lifetime values.  $^1\text{O}_2$  signal amplitudes were fitted by analysis of the data using the FluoFit 4.0 software.  $\Phi_{\Delta}$  values were calculated using Equations S1 and S2. All the  $^1\text{O}_2$  signals shown are background-corrected.

## Supporting Information

$$S(t) = S(0) \cdot \frac{\tau_{\Delta}}{\tau_T - \tau_{\Delta}} \cdot \left( e^{-t/\tau_T} - e^{-t/\tau_{\Delta}} \right) \quad \text{Equation S1}$$

$$\Phi_{\Delta}(\text{sample}) = \Phi_{\Delta}(\text{ref}) \cdot \frac{\left( \frac{S(0)}{(1 - 10^{-Abs})} \right)_{\text{sample}} \cdot \left( \frac{\tau_T - \tau_{\Delta}}{\tau_{\Delta}} \right)_{\text{sample}}}{\left( \frac{S(0)}{(1 - 10^{-Abs})} \right)_{\text{ref}} \cdot \left( \frac{\tau_T - \tau_{\Delta}}{\tau_{\Delta}} \right)_{\text{ref}}} \quad \text{Equation S2}$$

Indirect measurement of  $^1\text{O}_2$  was performed using uric acid (UA) as a chemical probe as recently described.<sup>6</sup> Absorbance values at 292 and 315 nm were measured vs irradiation time of optically-matched solutions of FMN or miniSOG and 50  $\mu\text{M}$  UA at 450 nm, and degradation rates were compared. Upon reaction with  $^1\text{O}_2$ , UA forms a hydroperoxide intermediate that undergoes additional ( $^1\text{O}_2$ -independent) reaction steps to final degradation products such as triuret, urea and cyanuric acid.<sup>7</sup>



**Scheme S1.** Photosensitized oxygenation of UA showing hydroperoxide intermediates (adapted from ref. <sup>7</sup>)

As a result, absorbance at 292 nm decays with biexponential kinetics. As the degradation of the hydroperoxide intermediate is oxygen-independent, only the first decay ( $k_1$ ) reflects the reaction with singlet oxygen. The reaction can also be monitored at 315 nm, with the difference that the intermediate formation ( $k_1$ ) appears as an increase of absorbance.<sup>6</sup> Panels a and b in Figure S3 compare UA degradation due to photoexcited FMN and miniSOG, respectively.

## Supporting Information

### Deuterium isotope effect on the photooxidation of ADPA

The finding that in dPBS the ratio of ADPA photooxidation rates decreased to *ca.* 1/3 can be rationalized bearing in mind that since the lifetime of singlet oxygen is longer in dPBS, the rate of ADPA photooxidation by singlet oxygen increases in dPBS (see Equation S3):

$$v_{\text{-ADPA}} = v_{\Delta} \times \frac{k_r[\text{ADPA}]}{\frac{1}{\tau_{\Delta}^0} + k_q[\text{ADPA}]}$$

Equation S3

where  $v_{\Delta}$  is the rate of singlet oxygen production,  $k_r$  is the photooxidation rate constant,  $\tau_{\Delta}^0$  is the lifetime of singlet oxygen in the neat solvent and  $k_q$  is the rate constant for the overall scavenging of singlet oxygen by ADPA (oxidation plus quenching).

Thus, if FMN would act via singlet oxygen but miniSOG would not, the photooxidation rate  $v$  would increase only for FMN and the ratio  $v_{\text{miniSOG}}/v_{\text{FMN}}$  would be smaller in dPBS than in PBS, as observed.

### ADPA photooxidation studies

The contribution of electron-transfer processes to the miniSOG-sensitized photooxidation of ADPA was further supported by laser flash photolysis experiments. When oxygen-depleted solutions of miniSOG or FMN were blue-irradiated in the presence of increasing amounts of ADPA, formation of new long-lived transient species could be readily observed in both cases, whose absorbance increased in an ADPA-concentration dependent manner (Figure S5). We attribute these new species to semioxidized forms of ADPA, in line with previous reports for other anthracene derivatives.<sup>8</sup> In addition, we observed that, in the presence of ADPA, the fluorescence of miniSOG was partially quenched and the spectrum lost its vibronic structure (Figure S6). This suggests that ADPA binds to miniSOG, as observed for other anthracene derivatives,<sup>9,10</sup> which facilitates the electron-transfer process.

The results above indicate that photooxidation of ADPA results from both  $^1\text{O}_2$ -dependent and -independent processes, the latter facilitated by the binding of ADPA to the protein.

## Supporting Information

### Supporting Figures

**Figure S1.** Triplet state kinetics of miniSOG and FMN.

**Figure S2.** Photodynamic bacterial inactivation studies.

**Figure S3.**  $\Phi_{\Delta}$  measurements using UA as a  $^1\text{O}_2$  probe.

**Figure S4.** ADPA photobleaching with an electron transfer photosensitizer.

**Figure S5.** MiniSOG, FMN and pyrylium electron transfer photoreactivity with ADPA.

**Figure S6.** ADPA interaction with miniSOG followed by steady-state fluorescence.

**Figure S7.** MiniSOG spectral behavior upon denaturation

**Figure S8.** Tagless miniSOG spectral behavior upon cumulative irradiation

**Figure S9.** FMN spectral behavior and  $\Phi_{\Delta}$  changes upon cumulative irradiation

## Supporting Information

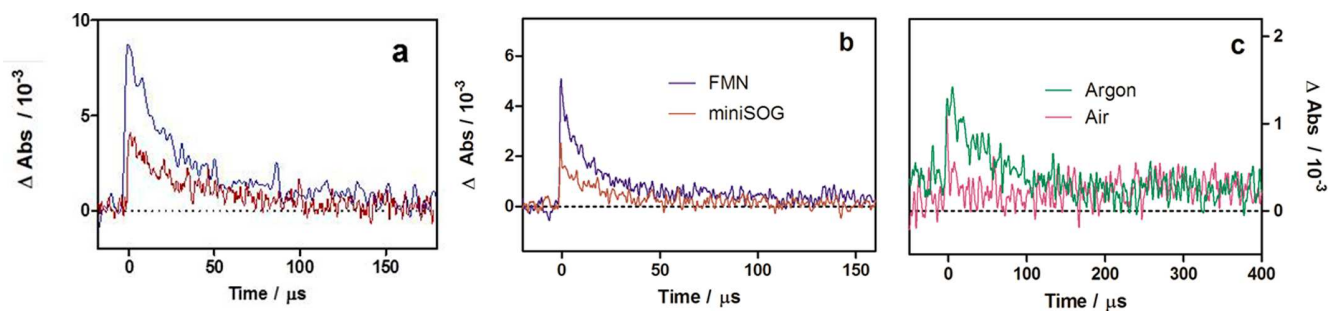


**Figure S1.** Transient absorption decays of FMN (blue line) and miniSOG (red line) observed at 300 nm (a) and 700 nm (b) for argon-saturated optically-matched solutions excited at 355 nm. Transient absorbance decays for argon-saturated solutions (green line) or aerated solutions (pink) of miniSOG observed at 300 nm and excited at 475 nm (c).

## Supporting Information

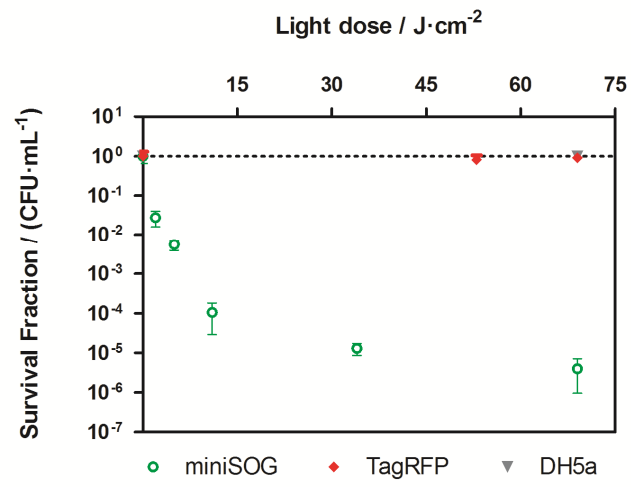


**Figure S2.** Comparison of *E. coli* light-dose dependent photokilling effect of TagRFP and miniSOG upon irradiation with green or blue light, respectively. Experiments were carried out in triplicate for each condition.

## Supporting Information

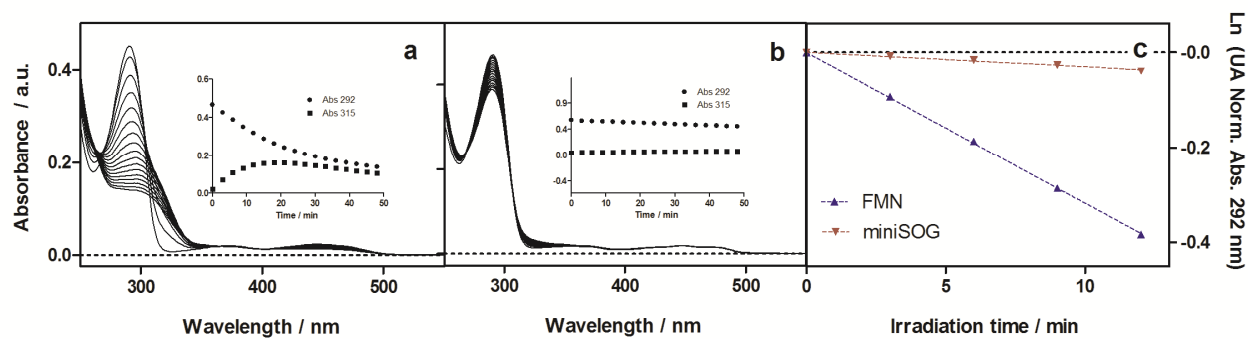


**Figure S3.** Singlet oxygen quantum yield determination using UA as probe. Spectral variations of optically-matched solutions of FMN (a) and miniSOG (b) in the presence of UA 50  $\mu\text{M}$  upon excitation at 450 nm. Insets: time-dependent absorbance variations at 292 and 315 nm. (c) Comparison of UA bleaching rate at 292 nm in the presence of miniSOG (red) or FMN (blue).

## Supporting Information

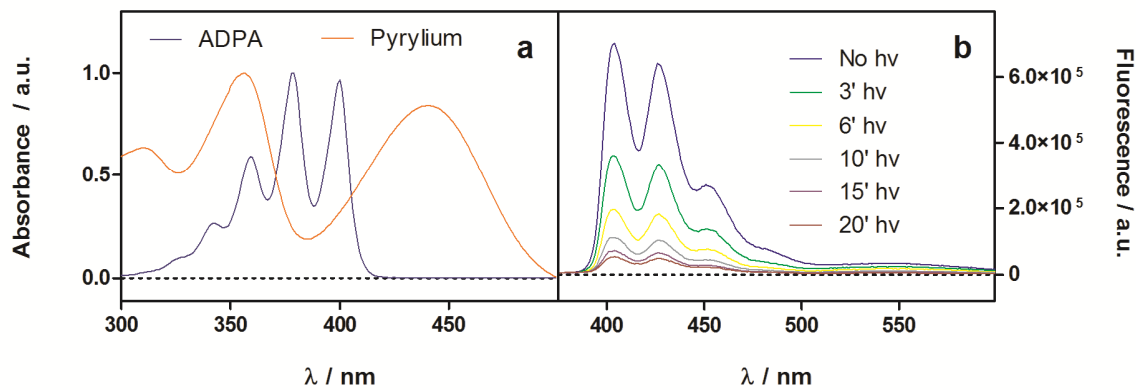


**Figure S4.** (a) Absorption spectra of ADPA (blue) and 2,4-diphenyl-6-(4'-methoxyphenyl)pyrylium tetrafluoroborate (Pyrylium; orange). (b) ADPA fluorescence photobleaching upon blue light irradiation in the presence of Pyrylium. Fluorescence was acquired at  $\lambda_{\text{exc}} = 355$  nm.

## Supporting Information

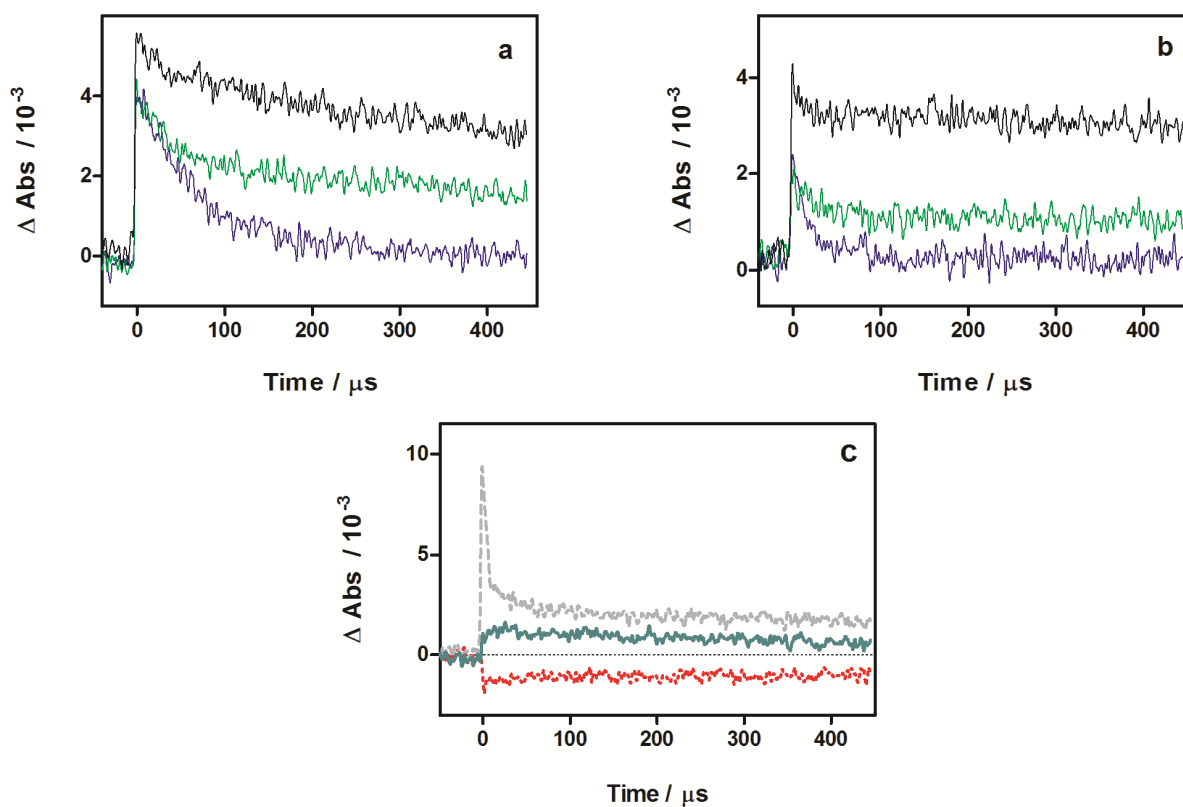


**Figure S5.** Transient absorption of (a) FMN, (b) miniSOG and (c) the electron acceptor pyrylium in deaerated PBS solutions in the presence of ADPA. For FMN and miniSOG  $\lambda_{\text{exc}} = 475 \text{ nm}$  (and traces correspond to increasing amounts of ADPA: 0  $\mu\text{M}$ , blue line; 12  $\mu\text{M}$ , green line; 60  $\mu\text{M}$ , black line; In panel c, the red trace corresponds to pyrylium alone, green to ADPA alone, and grey to their combination (12  $\mu\text{M}$  ADPA);  $\lambda_{\text{exc}} = 355 \text{ nm}$ . In all cases  $\lambda_{\text{obs}} = 300 \text{ nm}$ .

## Supporting Information

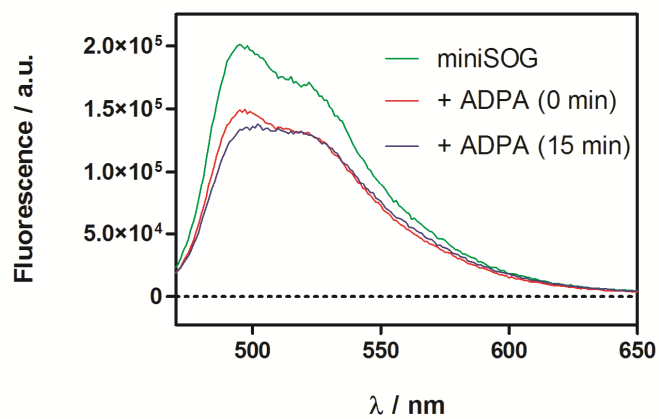


**Figure S6.** MiniSOG fluorescence time-dependent changes upon addition of 20  $\mu\text{M}$  ADPA. Fluorescence was acquired at  $\lambda_{\text{exc}} = 450 \text{ nm}$ .

## Supporting Information

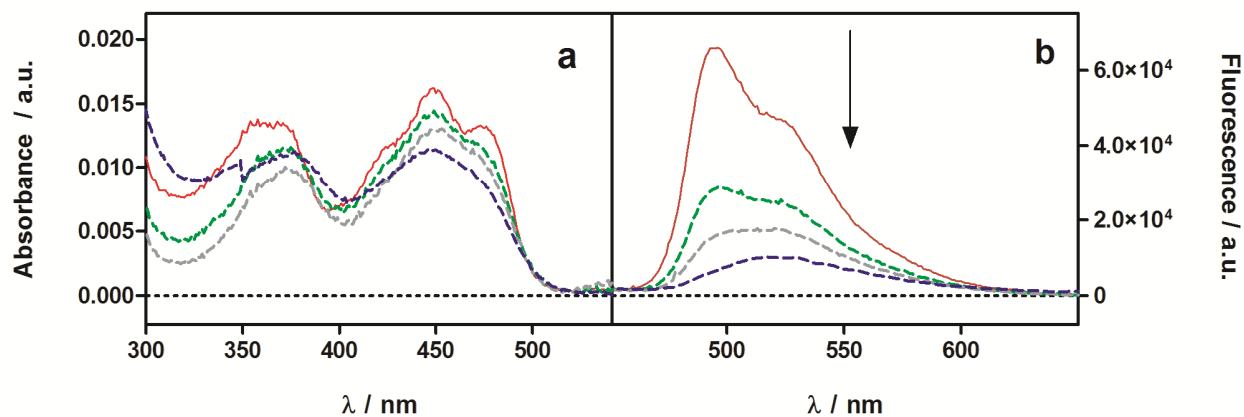


**Figure S7.** Absorption (a) and fluorescence (b) spectral changes of 2.5  $\mu\text{M}$  miniSOG in Gdn HCl 6 M PBS over time (solid red line corresponds to initial measurement; green, grey and blue dashed lines correspond to contact times of 60, 105 and 250 min). Fluorescence was acquired at  $\lambda_{\text{exc}} = 355$  nm. The initial resolved vibronic structure of miniSOG is progressively lost as the protein denatures and FMN is released. Note that, unlike other flavoproteins, denaturation results in loss of fluorescence as free FMN has a lower fluorescence quantum yield than miniSOG.

## Supporting Information

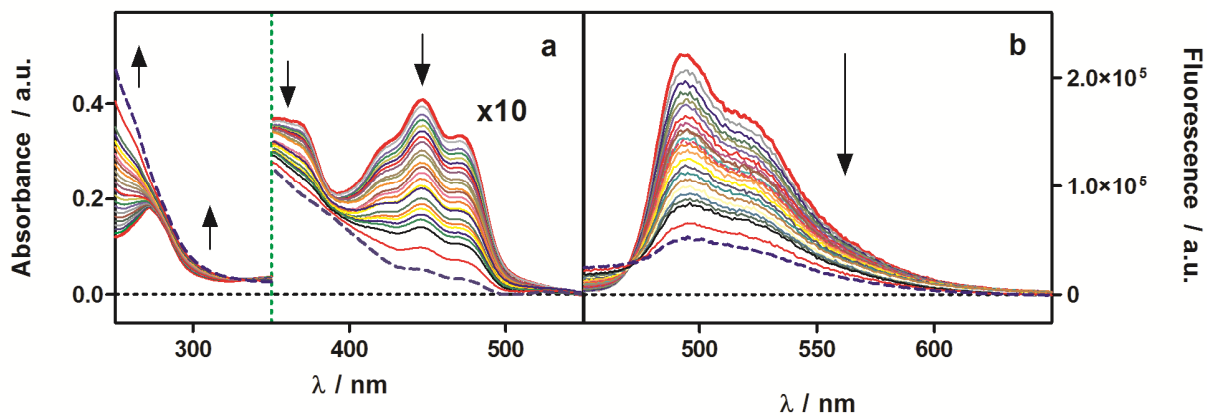


**Figure S8.** Absorption (a) and fluorescence (b) changes of 2.5 μM tagless miniSOG in dPBS upon cumulative irradiation at  $\lambda_{\text{exc}} = 355$  nm.

Fluorescence was acquired at  $\lambda_{\text{exc}} = 400$  nm.

## Supporting Information

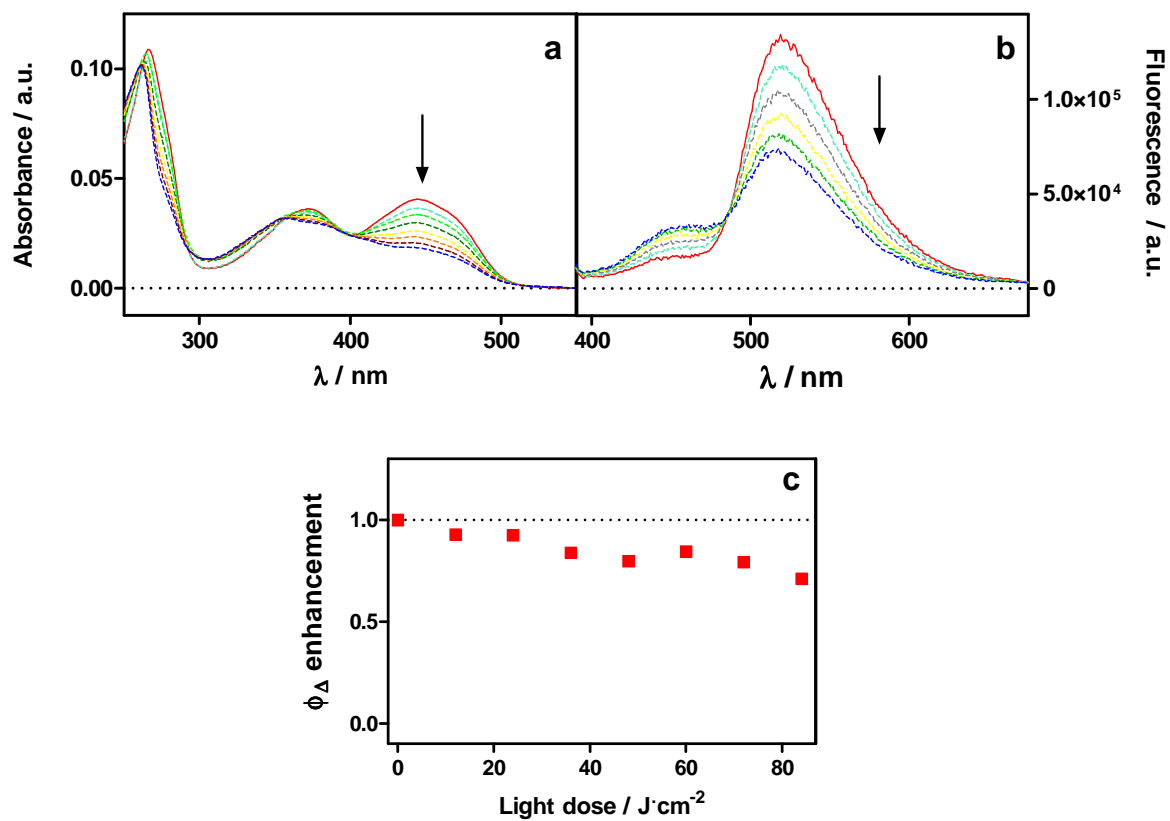


**Figure S9.** Absorption (a) and fluorescence (b) changes of FMN in dPBS upon cumulative irradiation at  $\lambda_{exc} = 355$  nm. Fluorescence was acquired at  $\lambda_{exc} = 355$  nm. (c) Relative enhancement of  $\Phi_{\Delta}$  values taking into account absorbance decrease.

## Supporting Information

### Supporting references

1. Nonell, S.; González, M.; Trull, F. R. *Afinidad* **1993**, *50*, 445-450.
2. Shaner, N. C.; Campbell, R. E.; Steinbach, P. A.; Giepmans, B. N. G.; Palmer, A. E.; Tsien, R. Y. *Nat Biotech* **2004**, *22*, 1567-1572.
3. Shu, X.; Lev-Ram, V.; Deerinck, T. J.; Qi, Y.; Ramko, E. B.; Davidson, M. W.; Jin, Y.; Ellisman, M. H.; Tsien, R. Y. *PLoS Biol.* **2011**, *9*, e1001041.
4. Munro, A.; Noble, M. In *Flavoprotein Protocols*; Chapman, S. K., Reid, G. A., Eds.; Humana Press Inc.: Totowa, NJ, 1999; Vol. 131, pp 25-48.
5. Jiménez-Banzo, A.; Ragàs, X.; Kapusta, P.; Nonell, S. *Photochem. Photobiol. Sci.* **2008**, *7*, 1003-1010.
6. Rabello, B. R.; Gerola, A. P.; Pellosi, D. S.; Tessaro, A. L.; Aparicio, J. L.; Caetano, W.; Hioka, N. *J. Photochem. Photobiol. A.* **2012**, *238*, 53-62.
7. Matsuura, T.; Saito, I. *Tetrahedron* **1968**, *24*, 6609-6614.
8. Shida, T. *Electronic absorption spectra of radical ions*; Physical sciences data; Elsevier science publishers: 1988; Vol. 34, pp 1-446.
9. Wilson, A. J.; Hong, J.; Fletcher, S.; Hamilton, A. D. *Org. Biomol. Chem.* **2007**, *5*, 276-285.
10. Wilson, A. J. *Chem. Soc. Rev.* **2009**, *38*, 3289-3300.